Bulletin of Engineering Geology and the Environment (2019) 78:3969–3981
https://doi.org/10.1007/s10064-018-1410-7

ORIGINAL PAPER

Influence of the petrophysical and durability properties of carbonate rocks on the deterioration of historic constructions in Tebessa (northeastern Algeria)

Fatah Nasri[1] · Abderrahmane Boumezbeur[2] · David Benavente[3]

Received: 16 May 2018 / Accepted: 13 October 2018 / Published online: 27 October 2018

Abstract

A thorough investigation of the weathering phenomena affecting a Byzantine Wall has been carried out. This Wall is a representative example of historic constructions in Tebessa (northeastern Algeria), in which limestone and carbonate tufa were the main materials used. Field investigations showed several weathering forms, including flaking, alveolisation, efflorescence, discolouration, fracturing, material loss and powdering. These weathering forms were mainly produced by salt action (gypsum and halite) and were related to the textural and petrophysical properties of the limestone and carbonate tufa. The quantification of the degree of deterioration using a Schmidt hammer revealed damage ranging from medium to severe. Petrophysical and durability properties were measured for both stone types extracted from ancient quarries. Pore structure, capillarity imbibition, P wave velocities and uniaxial compressive strength were used to characterise the petrophysical properties of the stones, and salt crystallisation tests were used to estimate their durability. These properties are closely linked to the stone microstructure. Carbonate tufas show excellent durability under salt crystallisation and a lower mechanical strength than limestone. Limestone, on the other hand, despite its low porosity and better mechanical strength, shows lower durability values. While micropores contribute to the relatively lower durability values of limestone, in tufa, macropores reduce the salt crystallisation effectiveness and improve the durability. According to our investigation, the Byzantine Wall requires urgent preservation measures. In the built heritage of Tebessa, limestone is expected be more prone to deterioration than carbonate tufa.

Keywords Weathering · Degradation · Salt crystallisation · Limestone · Tufa

Introduction

This research is concerned with the study of the ongoing decay and degradation of the Byzantine Wall, which surrounds what was once Thevest, modern-day Tebessa, which is situated in the northern Aures Mountains in northeastern Algeria (Fig. 1a). Many weathering forms are clearly visible in the studied structure, ranging from slight discolouration up to the loss of material and granular disaggregation. At present, no deep investigation has been carried out to study the weathering damage of the Byzantine Wall. In this work, our goal is to characterise the extent to which differences in the properties of limestone and carbonate tufa lead to differences in weathering characteristics, including the identification of the main deteriorating agents. To demonstrate the effects of complex features such as bioturbation, fissures, micro- and macroporosity on stone durability, physical, morphological properties and salt crystallisation tests have been carried out.

✉ Fatah Nasri
nasri.fatah@umc.edu.dz

Abderrahmane Boumezbeur
boumezbeura@yahoo.fr

David Benavente
david.benavente@ua.es

[1] Laboratoire de géologie et environnement, Faculté des sciences de la Terre, de la Géographie et de l'Aménagement du Territoire, Université des Frères Mentouri Constantine 1, Route de Aïn-El-Bey, 25000 Constantine, Algérie

[2] Laboratoire Environnement Sédimentaire et Ressources Minérales et hydriques de l'Algérie orientale, Faculté des sciences, Université Larbi Tébessi, Tébessa, Algérie

[3] Departamento de Ciencias de la Tierra y el Medio Ambiente, Universidad de Alicante, Ap. 99, 03080 Alicante, Spain

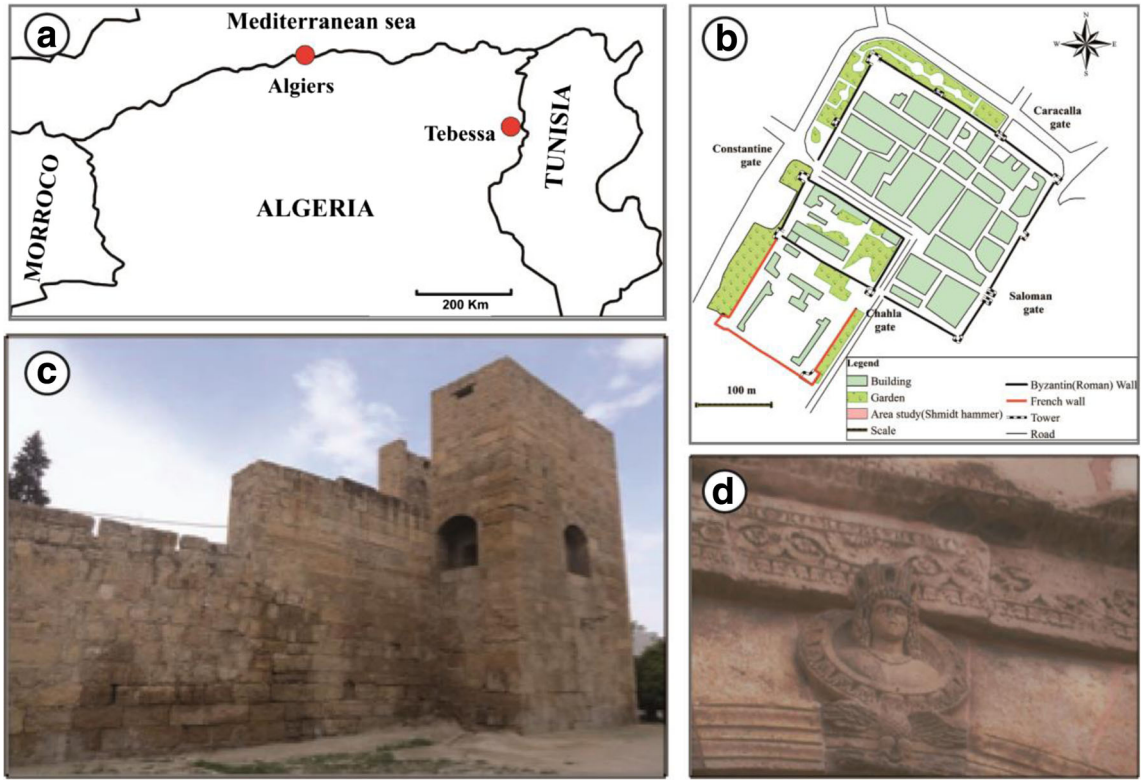

Fig. 1 Location of Tebessa in northeastern Algeria (**a**) , schematic map of the Byzantine Wall including the location of the study area into the north facade (**b**), the north part of the Byzantine Wall (**c**) , and a statuette of Septimus Emperor Wife's in the Caracalla Gate (**d**)

Since ancient times, monuments have been widely constructed with carbonate rocks, which are the most used rocks for construction in the world due to their high availability (Goudie and Viles 1997; May 1997; Török 2006; McCabe et al. 2007; Cassar et al. 2011; Espinosa-Marzal and Scherer 2010; Smith et al. 2010; Garcia-Guinea et al. 2013; La Russa et al. 2013; Ruffolo et al. 2015a, b). During the Roman occupation of North Africa, many monuments, such as the Byzantine Wall, the Basilica, the Temple of Minerve and many more in Tebessa, were constructed with carbonate rocks. Like all rocks, the stones of monument walls have been subjected to weathering by the atmosphere and hydrosphere since their exhumation.

In the context of construction material weathering and decay in historical monuments, a great deal of research has been undertaken to identify and understand the agents and mechanisms of degradation to devise better practices for eventual restoration procedures. In many instances, when restoration works have been undertaken without a prior understanding of the degradation process, the restoration has aggravated the decay (Přikryl et al. 2010; Boumezbeur et al. 2015). It is thus worth conducting a deeper investigation into the nature of weathering and the agents causing it. Several weathering forms, such as flaking, efflorescence, exfoliation and granular disaggregation, demnonstrate the state of stone weathering and deterioration in built environments (Schaffer 1932; Price 1975, 2006, 2007; Winkler 1997; May 1997, 1998a; Doehne and Price 2010; Ruffolo et al. 2013, 2015a, 2015b; Emmanuel and Levenson 2014; Boumezbeur et al. 2015). In fact, the petrophysical properties of rocks are determined by their mineralogy and structure (Ruedrich et al. 2011); in turn, these complex properties are reflected in the stone weathering responses to the natural and built environments (May 1994, 1997, 1998b; Kramar et al. 2010).

Salt damage is considered a common hazard, playing a major role in the decay of stones under a wide range of environmental conditions (Goudie and Viles 1997; Doehne 2002; Gôtze and Siedel 2004), including the semi-arid region of NE Algeria where the Byzantine Wall is located. The durability of carbonate rocks is controlled mainly by soluble salt (Ruffolo et al. 2015b; Al Omari et al. 2016). Salt damage is controlled by multiple stone properties, and their actions occur through physicochemical reactions (Charola 2000). Thus, pore size distribution can strongly control the transport of liquids, which influences the stability of stones through the growth of their crystals and the pressure generated on the porous networks in the walls (Nicholson 2001; Benavente et al. 2007b; Yu and Oguchi 2010; Koniorczyk and Gawin 2012; Ruffolo et al. 2015b). According to López-Doncel et al. (2016), pore size distribution controls the effects of salt damage in stones, and stone durability is mainly related to the proportion of micropores. However, the petrophysical

properties of rocks change with the presence of fissures, which give rocks a double porosity response (Benavente et al. 2007b). In particular, the action of salt crystallisation in bioturbated zones in stone causes the development of alveoli close to the stone's surface (Cassar 2002). Limestone and carbonate tufa in the Byzantine Wall consist mainly of calcite, but they present contrasting weathering behaviours in response to the significant variations in their structure and texture (Kramar et al. 2010).

Materials and methods

Study site and stone materials

In 146 BCE, Tebessa became part of the Roman Empire with the name Thevest. Since that time, several buildings have been erected, such as the amphitheatre, the Temple of Minerve, the Arch of Caracalla, the Basilica and the Roman Wall. The latter was destroyed and rebuilt in the sixth century by the Byzantine General Solomon for security and political purposes (Castel 1912), and, as a result, the Wall is now called the Byzantine Wall. It is rectangular in shape; and spans 298 m in length, 260 m in width, and is 7 m high. The Byzantine Wall, which surrounds the city, contains four gates and fourteen square towers for surveillance (Fig. 1b, c). The main gate, the Caracalla Gate, was erected in 214 AD, faces north (Fig. 1d) and since 1982 has been classified as one of the cultural heritage treasures of the world. The Byzantine Wall was built entirely of carbonate stones and exhibits severe decay in its northern and western facades.

Carbonate sedimentary rocks are widespread in the Tebessa area, with the oldest outcrops being Albian, while the most recent outcrops are Quaternary (Durozoy 1953) (Fig. 2a). For rock monuments, the most used stratigraphical units are those of the middle Turonian for the limestone and the actual formation for the carbonate tufa (Coquand 1862). Limestone and tufa are the main rock types that were used as building materials for the Byzantine Wall. Hence, these materials are selected in this study due to their prevalence in the Wall and due to their wide range of weathering intensities. The limestone is pinkish in colour, middle Turonian in age and contains intensive bioturbations that are highly stained by iron oxides. The iron surfaces often show a few dolomite crystals. The petrographical analysis of the stones reveals that the main mineral component is calcite, which is accompanied by bioclasts and small percentages of quartz, dolomite and goethite (Fig. 2e). The observed bioclasts are the debris of lamellibranches and the spicules of echinoids, millioles, ostracods and gastropods. Recrystallised calcite grains range in size from 80 to 200 μm and sometimes reach 750 μm. Automorphic dolomite crystals have a diameter of 250–400 μm with a clear growth zone impregnated by iron oxides. These crystals are clearly seen as red patches in the bioturbation structures. This limestone presents vuggy and fissural porosity. According to Allag (2016), clay minerals such as montmorillonite and kaolinite can be observed in the Turonian limestone.

Carbonate tufa is another stone that is used in the Wall and is extracted from nearby quarries close to the monuments. The tufa is mainly composed of calcite and is deposited by springs, which were common near the city of Thevest (Durozoy 1953). Tufa is a very porous, soft and spongy rock that often shows plant moulds (Fig. 2d). Tufa can be easily cut and reworked into cubic blocs. Generally, tufa is commonly formed by the precipitation of calcite from normal freshwater in lakes and shallow ponds. This carbonate tufa has an arborescent texture and a complex structure.

Methods

Fresh stones (quarries)

Fresh stones were sampled from the ancient Roman quarries assumed to be quarried for the construction of the Byzantine Wall and other monuments (Coquand 1862). Carbonate tufa was extracted from the quarry of Djebel Djoua (Fig. 2b), which is located approximately 1 km east of the Byzantine Wall, while fresh limestone was extracted from an ancient quarry in Djebel Doukkane (Fig. 2c), which is located approximately 6 km WSW.

Petrophysical and durability characterisations were carried out on representative fresh limestone and carbonate tufa samples. This characterisation is essential to understand the stone behaviours under different factors and their properties, which play a great role during the weathering process. Pore sizes were measured on unweathered samples to determine the petrophysical properties of the studied rocks. These properties were open porosity, capillary imbibition and P wave velocity. Porosity and ultrasonic wave velocity were measured a second time after durability tests to evaluate the changes in the rock properties.

Total porosity, ϕ_T, defined as the ratio of the total volume of pore space to the bulk material volume, is calculated using the relationship between the bulk and grain densities. Bulk density, ρ_{bulk}, was determined through direct measurements of the dried weights and dimensions of samples. The grain, or real density, ρ, of a material is defined as the ratio of its mass to its solid volume. Both

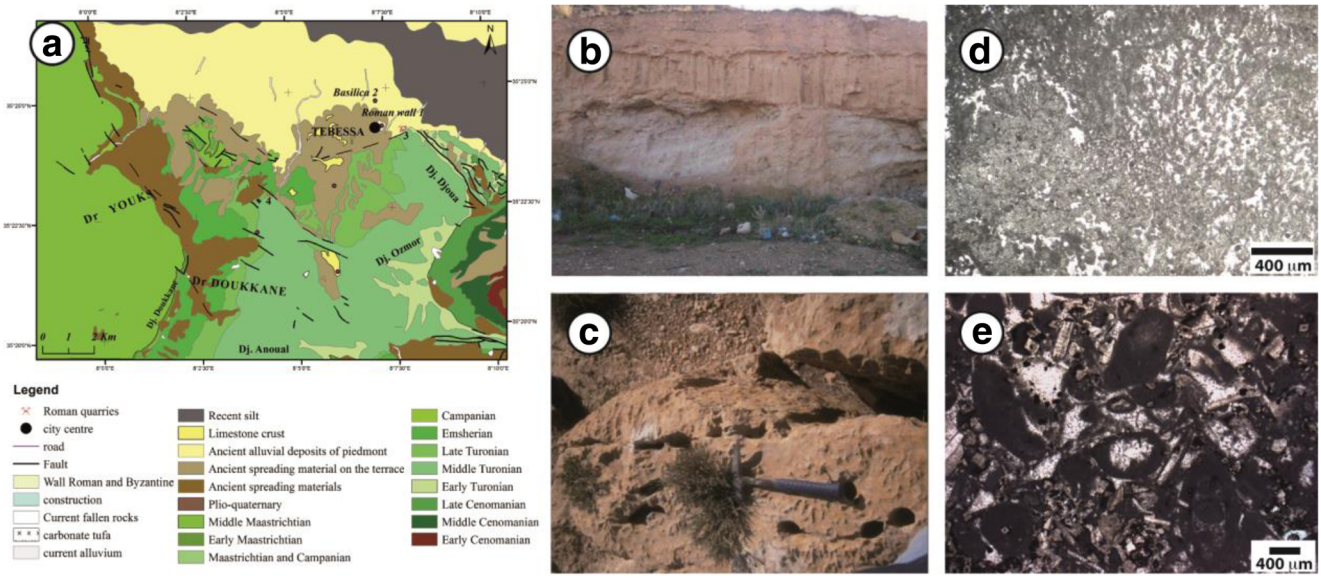

Fig. 2 Geological map of Tebessa (Durozoy 1953) (**a**) and the view of the tufa quarry in Djebel Djoua (**b**) and the limestone quarry in Djebel Doukkane (**c**). Optical microphotographs of carbonate tufa (**d**) and limestone (**e**) textures

stones are composed of calcite (more than >98%); therefore, the grain density was considered to be the density of calcite (2.71 g/cm^3). Open porosity, ϕ_O, was obtained using the vacuum water saturation test (UNE-EN 1936 2007). The connected porosity, ϕ_c, and pore size distribution were calculated via the mercury intrusion porosimetry (MIP) technique. A PoreMaster 60 GT (Quantachrome Instruments) mercury porosimeter was used, and a surface tension and contact angle of mercury of 480 mN/m and 130°, respectively, were chosen. The pore radius interval ranges from 0.002 to 200 µm, which corresponds to the highest and lowest head pressures, and, consequently, MIP cannot characterise large vug pores. The samples used are prismatic in shape and have a size of 0.216 cm^3.

Capillary absorption coefficients, C, were determined using the standard method for limestone in accordance with UNE-EN-1925 (1999). The continuous method was used to characterise tufa varieties because of their high absorption rates ($C > 150$ g/m^2 s$^{0.5}$) (Benavente et al. 2007a). To analyse the capillary water absorption, six cubic samples of 5 cm each were cut for every stone type. These specimens were soaked in approximately 0.2 cm of water. For data acquisition, weight measurements were taken every 30 s for the carbonate tufa until sample saturation was achieved (approximately 10 min). For the limestone, weight measurements were taken every 3 min for the first hour, then every 1 h for 8 h, and then 1 measurement was taken every day up to the 7th day. The capillary absorption coefficient was calculated from the weight increase per unit area versus the square root of time. The results were plotted as the mass of water absorbed per area of sample during imbibition versus the square root of time.

P wave velocities, v_P, were measured using signal emitting–receiving equipment (NDT 5058PR; Panametrics,) and an oscilloscope (TDS 3012B; Tektronix). The uniaxial compressive strength, σ_C, was evaluated according to the standard test EN-1926 (2007) using a servo-controlled compression machine with a loading capacity of 200 kN.

The mineral compositions of both stones (limestone and tufa) in their fresh states were determined by X-ray diffraction (XRD) on a powder of a crushed sample (63 µm size) using a Philips PW 1840 diffractometer, and the patterns were run with Ni-filtered Cu Kα radiation ($\lambda = 1.54056$ Å) at 40kv and 10 mA. The scanning range was from $2\theta = 1$ to 80°. To characterise the microtextural properties of the stones, the limestone and tufa were examined with a scanning electron microscope (SEM), and SEM microprobe analyses were performed by an SEM JEOL JSM 6400 coupled with an energy dispersive X-ray spectrometer (EDX) system, detector model 6587, to identify the textural and mineralogical composition of rocks. The samples were coated with gold under a 10-kV voltage.

Durability tests

The salt crystallisation test was carried out in accordance with EN-12370 (1999) recommendations. Cubic samples of the 4-cm side were cut from the studied stone types and soaked in a saline solution of 14% w/w Na_2SO_4 at 20 °C for 4 h, followed by a drying period at 105 °C for 16 h and cooling at 20 °C for 4 h. This test was repeated

for 15 cycles. The evolution of the open porosity, bulk density, P wave velocities and the dry weight loss, ΔW (%), were calculated at the 15th cycle after cleaning and oven-drying the samples. After each cycle, the weight of each sample was determined to an accuracy of ±0.01 g. The specimens were visually inspected to quantify the salt action.

Weathering characterisation

Weathering occurs because of the interactions of environmental factors with stone materials and consequently brings mineralogical, textural and morphological changes to the surface of the rock. The superficial alteration of the stone presents different weathering forms (Heinrichs 2008; Siedel et al. 2011). These weathering forms have been observed at the mesoscale (cm to metre), with different lengths and widths. To determine the weathering forms on the Byzantine Wall facades, the mapping techniques of Fitzner et al. (1995) and Siedel et al. (2011) were used, in which weathering damage is mapped and classified into different categories, where each shows the dominant weathering form, the intensity and the state of the monument preservation.

The study area is situated along the north part of the Byzantine Wall where the Wall face is clearly visible and accessible. This method was carried out on an area of approximately 20 m^2 of the Wall.

The Schmidt hammer test was carried out on the surface of the weathered and unweathered stones to establish the hardness values of their surfaces according to ISRM (1978) and ASTM (2001) recommendations. A Schmidt hammer provides an inexpensive and fast measure of the surface strength of the rocks, and is in fact a measure of the surface hardness of building stones (Queisser 1986, Schneider et al. 2008, Nazir et al. 2013). These values are widely used to estimate the effect of weathering on the mechanical properties of rock material (Schneider et al. 2008; Aydin 2009).

Weathered samples were extracted from the north and west facades of the Byzantine Wall, where the main weathering forms are the most representative. These samples were characterised by XRD and electron microscopy.

Results and discussion

Mineralogical and textural characterisation

The results of the XRD analysis of limestone and tufa show that the main mineral constituent is calcite, whereas the secondary minerals in this limestone are quartz, dolomite and goethite.

On the limestone, a brownish colour and fissures are widely exhibited on bioturbation surfaces. Inside the bioturbation structures, the brownish colour is the result of iron oxide (goethite), which was detected by the XRD analysis and supported by SEM observations (Fig. 3a). Under SEM, the fissures are of different lengths and widths without preferential orientation and are generally less than 200 μm in width. In this case, these fissures are assumed to be original. The fissure surfaces show the presence of clay minerals between the grains, which was detected by SEM (Fig. 3a) and confirmed by EDX microanalysis.

Under SEM observations, the porosity is more important in bioturbation structures than in other parts of the stone, and the porosity is below 200 μm (Fig. 3a); however, surfaces without bioturbation or fissures have pore radii of less than 10 μm. Intercrystalline porosity can be seen in this limestone and is related to the fissure surfaces and bioturbation. In particular, clay with a low thickness can play a role in cementing grains together and reducing the porosity. Additionally, in very porous media, clay deposited in intercrystalline spaces stops the circulation of water (Siegesmund and Török 2011). The arrangement and the spatial distribution of the fissures and bioturbations within the limestone seem to play an important role in the control of petrophysical and mineralogical properties. The presence of bioturbation, fissures and clay minerals inside the fissures plays a great role in the control of water movement, causing detachment, fracturation and swelling, respectively (Nicholson 2001; Jiménez González and Scherer 2004; Benavente et al. 2007a; Siegesmund and Dürrast 2011).

In carbonate tufa, however, plant moulds create macropore-scale pores and voids. The investigations of the carbonate tufa (Fig. 3b) show the presence of large pores that can reach 500 μm, as shown by the SEM observations. The significant interconnection between the pores in the carbonate tufa can result in high values of pore connectivity as well as in high capillary imbibition coefficients (García-del-Cura et al. 2012).

Petrophysical characterisation of fresh samples

The main agent of weathering and degradation of stones is water, which plays an important role in the transfer and deposition of particles within the stone (Beck and Al-Mukhtar 2010). For this purpose, petrophysical characterisation is essential for understanding the behaviour of stones and evaluating their durability. In fact, bulk density, porosity and pore size distribution influence rock susceptibility to weathering because nearly all the weathering processes rely on the chemical reactions of salts or other contaminants with the stone material in the porous media (Nicholson 2001). The petrophysical characteristics of

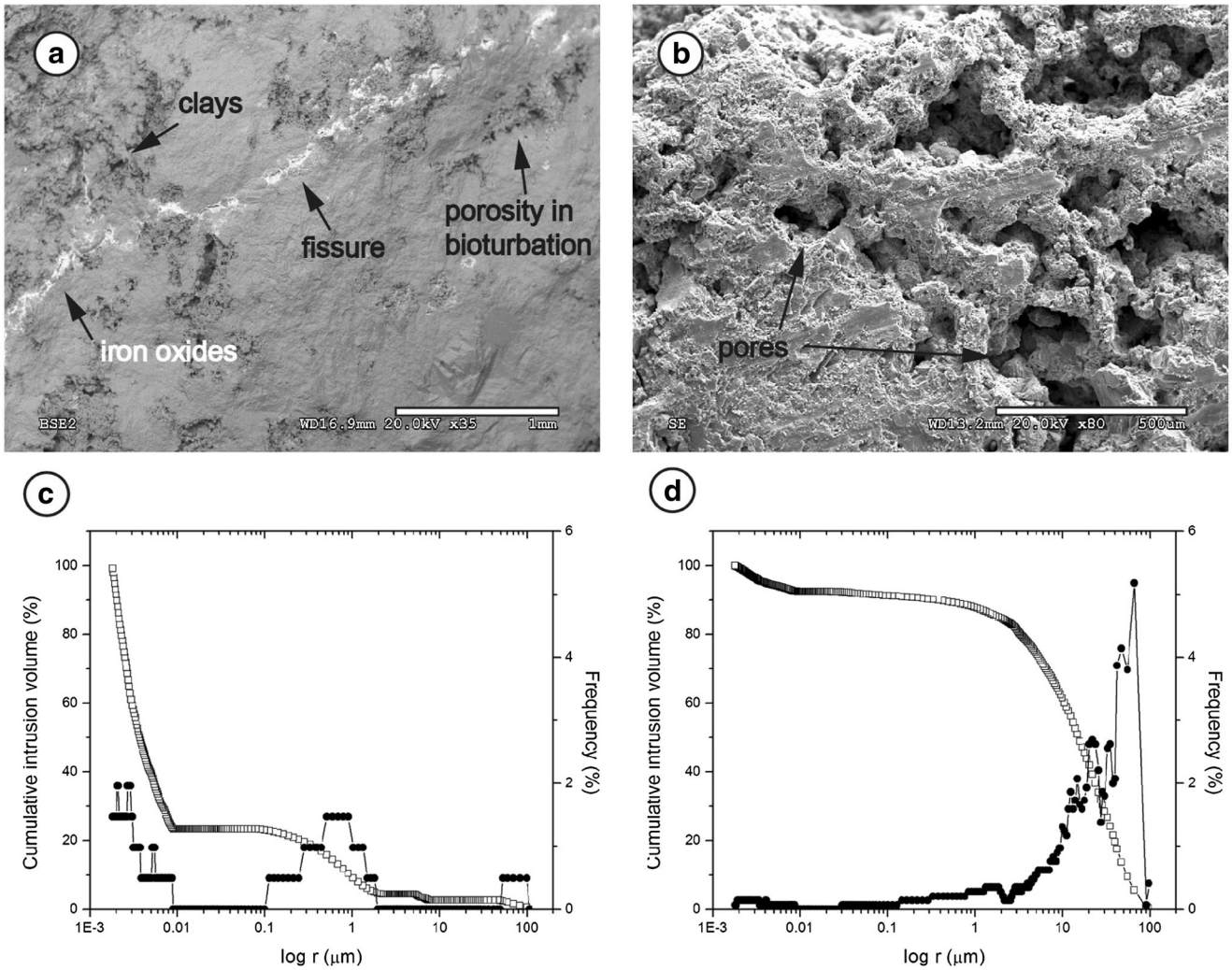

Fig. 3 Scanning electron microscope images (SEM) and pore size distribution of the investigated samples. The limestone structure shows: fissures, porosity in fissures, clays and iron oxides (**a**); the tufa structure shows porosities and their interconnection (**b**). Cumulative mercury intrusion curves and pore size distribution curves (MIP) for limestone (**c**) and carbonate tufa (**d**)

limestone and carbonate tufa are shown in Table 1. The porosity of carbonate tufa is more important than that of limestone because carbonate tufa is characterised by its macropore volume, which is reflected by the fact that the total porosity values are higher than the connected porosity values. The limestones, with a 2.58 ± 0.02 g/cm^3 bulk density, represent heavy samples, while the carbonate tufas, with a 1.47 ± 0.12 g/cm^3 bulk density, represent the lightest samples.

The presence of macropores in the stone is shown by significant mercury intrusions beyond the detection limit of MIP (García-del-Cura et al. 2012). MIP shows different porous networks between the limestone and the carbonate tufa. Figure 3c shows that the limestone exhibits a polymodal pore size distribution, where the thin pores (0.001-0.01 µm) represent 72% of the pore population. This kind of pore size distribution corresponds mainly to interparticle pores because the larger pores indicate the interparticle pores around bioturbations and fissures (Fig. 3a). In the carbonate tufa (Fig. 3d), the pore size distribution is mainly unimodal, in the range 1–100 µm, and its porosity can exceed 1 cm, which has been shown in macroscale investigations and is supported

Table 1 Petrophysical values of the limestone and carbonate tufa. ρ_{bulk} Bulk density, ϕ_O open porosity, ϕ_T total porosity, ϕ_c connected porosity, v_P compressional wave velocity, σ_C uniaxial compressive strength, *C* capillary absorption coefficient

	Limestone	Carbonate tufa
ρ_{bulk} (g/cm^3)	2.58 ± 0.02	1.47 ± 0.12
ϕ_O (%)	4.48 ± 1.02	44.37 ± 2.5
ϕ_T (%)	6.23 ± 0.83	54.82 ± 4.88
ϕ_c (%)	3.85	28.09
v_P (m/s)	5949 ± 139	3605 ± 249
σ_C (MPa)	63.71 ± 7.17	2.21 ± 0.58
C (g/m^{2}s$^{0.5}$)	3.28 ± 0.20	653.33 ± 197.69

by SEM observations (Fig. 3d). The connected porosity, ϕ_C, coincides with the open porosity in the limestone rocks but differs greatly in the carbonate tufa facies. When the micro- and the macropores are joined, the open porosity gives more realistic results for interpreting the porosity of the carbonate tufa (García-del-Cura et al. 2012).

The capillary absorption coefficient, C, of the limestone is less than that of the porous carbonate tufa, which reflects the pore networks of these stones (Table 1). Capillary imbibition occurs mainly in pore sizes between 1 μm and 1 mm and provides high water absorption rates for a well-connected pore structure (Benavente et al. 2007b, 2015). Thus, the large pores in carbonate tufas play a major role in the overall capillary absorption, as seen in the C–ϕ_o graph where the high porosity values show a high capillary absorption coefficient (Fig. 4a). The action of capillary transport is negligible for pore radii of up to 1 mm, and the mechanism that predominantly controls fluid movement is gravity. Hence, the large pores in carbonate tufa are revealed by the difference between the total and connected porosities. In fact, the main mechanisms that control the fluid in the carbonate tufa are capillary action and gravity, while capillary action is the main mechanism in the limestone.

The v_P–ϕ_T graph shows that P wave velocity increases when porosity decreases according to a linear relationship (Fig. 4b) (García-del-Cura et al. 2012). The propagation of ultrasonic waves is hindered in stones with high porosities. According to Martínez-Martínez (2008) and Martínez-Martínez et al. (2011), the lower v_P obtained for some samples of limestone can be explained by the presence of large calcite crystals inside the textures and the fissures. Limestone and tufa present medium to very low uniaxial compressive strengths according to Deere and Miller (1966), ranging from 56 to 70 MPa for limestone and from 1.5 to 3 MPa for carbonate tufa. The relationship between strength and porosity shows an exponential trend for both stones (Fig. 4c), where the porosity provides preliminary information on strength values (Török 2006; García-del-Cura et al. 2012).

Porosity values of less than 10% indicate interparticle pores (intercrystalline and intergranular), while values higher than 45% are associated with macropores; thus, stone strength is more sensitive to macropores than to interparticle porosity (García-del-Cura et al. 2012; Benavente et al. 2018). These types of porosities highly influence the mechanical properties of stones in the sense that they determine the weakness of the structure. For low porosity rocks, small changes in porosity usually involve considerable changes in strength (García-del-Cura et al. 2012).

Durability test

Salt damage is the main mechanism responsible for stone weathering in the Byzantine Wall. Fresh limestone and carbonate tufa were subjected to an accelerated weathering process using the salt crystallisation test, which is widely used for stone durability assessments. The weathering of these stones was monitored using five parameters: (1) weight loss in the sample, (2) visual deterioration, (3) ultrasonic response, (4) bulk density and (5) open porosity. These parameters were studied to compare the variations in petrophysical values and to assess the degree of decay. Figure 5 shows the variation in weight loss after each cycle of the salt weathering test performed on the untreated samples. In general, the carbonate tufa presents excellent durability against salt crystallisation compared to that of the limestone, such that the tufa samples are structurally sound at the mesoscale, while the limestone samples show different types of weathering forms.

Due to the formation of salt crystals inside the pore spaces, some limestone samples initially display an increase in their weights until the sixth cycle. Other samples continued to increase in weight until the tenth cycle. From the seventh cycle onwards, the limestones show a decrease in weight and begin to degrade, exhibiting several weathering forms, such as efflorescence, fracture, flaking and loss of materials, mainly in

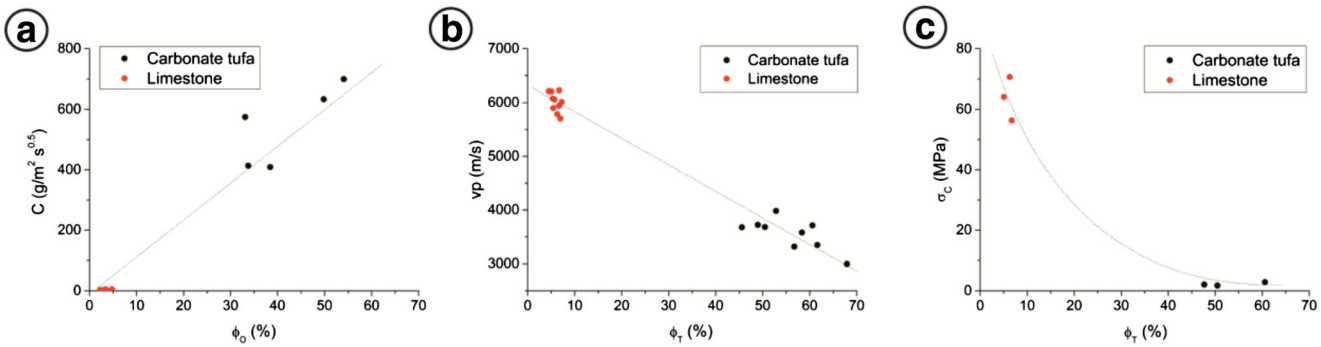

Fig. 4 The correlations of petrophysical properties. Capillary coefficient absorption versus open porosity (**a**), P wave velocities versus total porosity (**b**), and compressive strength versus total porosity (**c**) of limestone and carbonate tufa

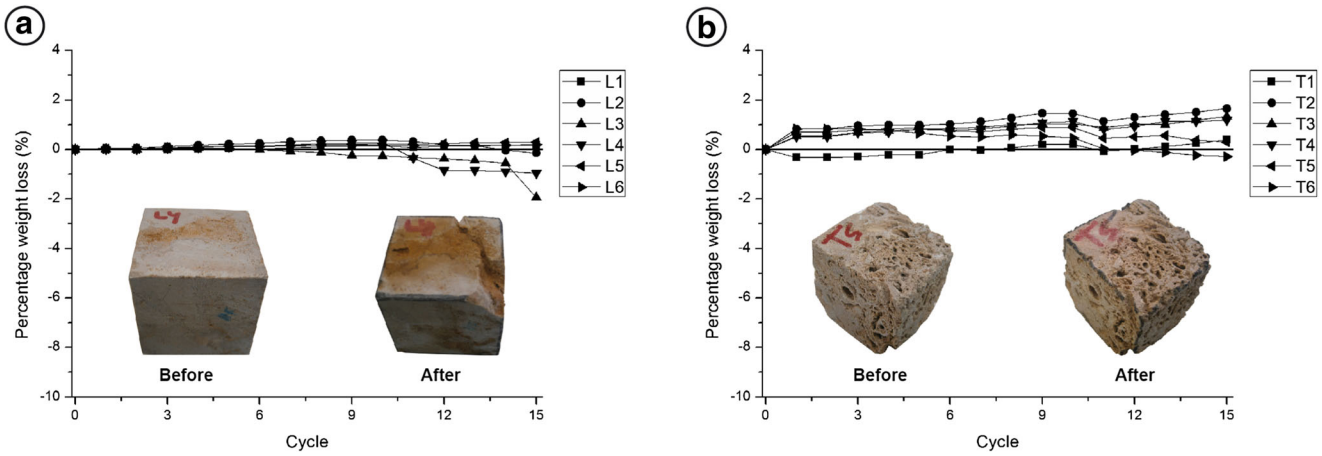

Fig. 5 Salt crystallisation test: curve representing the trend of weight loss of limestone (*L*) and carbonate tufa (*T*) during the 15 cycles of salt crystallisation, and their state before and after tests for limestone (**a**) and carbonate tufa (**b**)

the bioturbations (Fig. 5a). All the limestone samples display a superficial granular disaggregation, which contributes to the decrease in their weight after the durability test. In limestone, some superficial flaking is observed, which causes the loss of thick sheets on the sample surfaces. Fissures may coalesce and then turn into fractures and cause sample disaggregation and flaking. The formation of fissures and fractures involves both the initiation and propagation of pre-existing fissures or extensions of new fractures (Nicholson 2001), resulting in an increase in open porosity and a decrease in bulk density after the salt crystallisation test. Table 2 shows the variation of petrophysical properties after the salt crystallisation test. The variations are lower in both limestone and carbonate tufa. In limestone, this lower variation is controlled by fissures and loss of materials. An increase in fissure density also increases water absorption, which makes weathering more severe (Eppes and Keanini 2017). According to Thomachot and Jeannette (2002), wetting–drying cycles can increase the porous network density, which can lead to material damage.

Discolouration is another weathering form and can appear in the form of colour accentuation in bioturbation structures. Discolouration is caused by the reaction of iron oxides with water during the salt crystallisation test. The colours propagate around the bioturbation surface and result in the appearance of surface disaggregation. The presence of iron oxides associated with bioturbations increases local porosity and decreases rock strength because the chemical reactions between water and iron oxides through salt action lead to stone weakness and degradation. The influence of iron oxides on this type of weathering pattern has also been reported by Akin and Özsan (2011) and Benavente et al. (2018) in coloured travertine. The durability test shows the importance of this bioturbation, which is observed in the samples (L3 and L4) with high levels of bioturbation. As a consequence, these samples show more weathering, which is reflected in granular disaggregation and fracture formation. At the end of the test, the limestones show an average weight loss of approximately 1%.

In addition, the tufa samples show a sudden increase in weight after the first cycle because the amount of salt retained inside the stone is easily deposited without any detrimental effect (Fig. 5b). The stone undergoes no degradation, and a weight reduction is observed only in one sample, in which a small detachment on the surface is observed after the first cycle. The pressure generated by salt crystals is not sufficient to cause significant damage in this stone type because the pores are large enough to contain the pressures generated by salt growth, which can be seen from the fact that there is a 1% gain in weight. The decrease in the carbonate tufa porosity can be explained by the salt crystals that form inside the pore network, which is indicated by the decrease in bulk density (Table 2) and the increase in weight without weathering after the salt crystallisation test.

The mechanical strength evolution quantified by v_P is insignificant after the durability test, and, in most cases, the values fall between the maximum and minimum resistances of the unweathered samples (Table 2). Therefore, the more limited variation of the ultrasonic velocity corroborates that the internal changes alone (fissures and pores) are not sufficient to cause any deterioration in material properties. During the drying step of the test, the thermal expansion behaviour is at least partially controlled by single-crystal properties

Table 2 Petrophysical properties before and after the salt crystallisation test for the limestone and carbonate tufa. Bulk density, ρ_{bulk}; open porosity, ϕ_O; compressional wave velocity, v_P

	Limestone		Carbonate Tufa	
	Before	After	Before	After
ρ_{bulk} (g/cm^3)	2.58 ± 0.02	2.57 ± 0.02	1.47 ± 0.12	1.45 ± 0.14
ϕ_O (%)	4.48 ± 1.02	4.66 ± 0.98	44.37 ± 2.5	42.9 ± 4.38
v_P (m/s)	5949 ± 139	5916 ± 194	3605 ± 249	3600 ± 318

(Malaga-Starzec et al. 2002) because calcite strongly influences weathering due to the anisotropy of the coefficient of the thermal expansions of different mineral axes (Eppes and Griffing 2010). Therefore, the expansion and contraction of minerals within the stone induce the appearances of fissures and fractures, which weaken and accelerate weathering, especially in limestone with low porosity (Gomez-Heras et al. 2009; Benavente et al. 2018). Consequently, limestone and carbonate tufa present different decay mechanisms. Although the mechanical resistance of carbonate tufa is lower than that of limestone, tufa is more resistant to salt crystallisation action (Benavente et al. 2018). The resistance of the material to crystallisation pressure creates tensile stress over the pore surface (Benavente et al. 2004).).

However, the carbonate tufa exhibits larger pores (Fig. 3a), and thus, the weathering effect of salt pressure decreases considerably. Crystals may pass through large pores without generating significant levels of crystallisation pressure on the pore walls (Benavente 2011; Benavente et al. 2011). However, limestone has thin pores, where crystal growth produces an effective crystallisation pressure on the pore wall. The pressure generated by the growth of salt crystallisation produces a connection between isolated pores and open pores, which can enlarge fissures and create fractures (La Russa et al. 2013). A few clay minerals are also observed between calcite crystals and on surface fissures. Thus, both iron oxides and clay minerals may also enhance the effectiveness of salt crystallisation and contribute to granular disaggregation and fissuration.

Weathering characterisation

The Byzantine Wall of Tebessa exhibits a wide range of weathering forms that affect the main stones used in its construction (Fig. 6). Limestone has several weathering forms and generally presents soiling and efflorescence in the lower parts of the Wall. Efflorescence is related to water and fluid infiltration by capillary action, whereas soiling is caused by rainwater, which makes dust stick toi the lower parts of the stones. In particular, rising damp is a major problem of damage of the Byzantine Wall, which contributes to salt dissolution and transport through the pore structure of stones. Fissures affect some ashlars and are independent of limestone structure. At a height of 60 cm above the ground, the limestone mainly presents flaking, white crust, back weathering, alveolisation, discolouration and scaling (Fig. 6). Flaking is related to alveolisation, which is a step in the process of the formation of alveoli (Cassar 2002). Discolouration is associated with bioturbation and is widely found on the limestone surfaces because their bioturbations are rich in iron oxides. Moreover, the chemical erosion of these bioturbation structures affects the calcite and iron fractions prior to discolouration. The bioturbation surfaces show granular

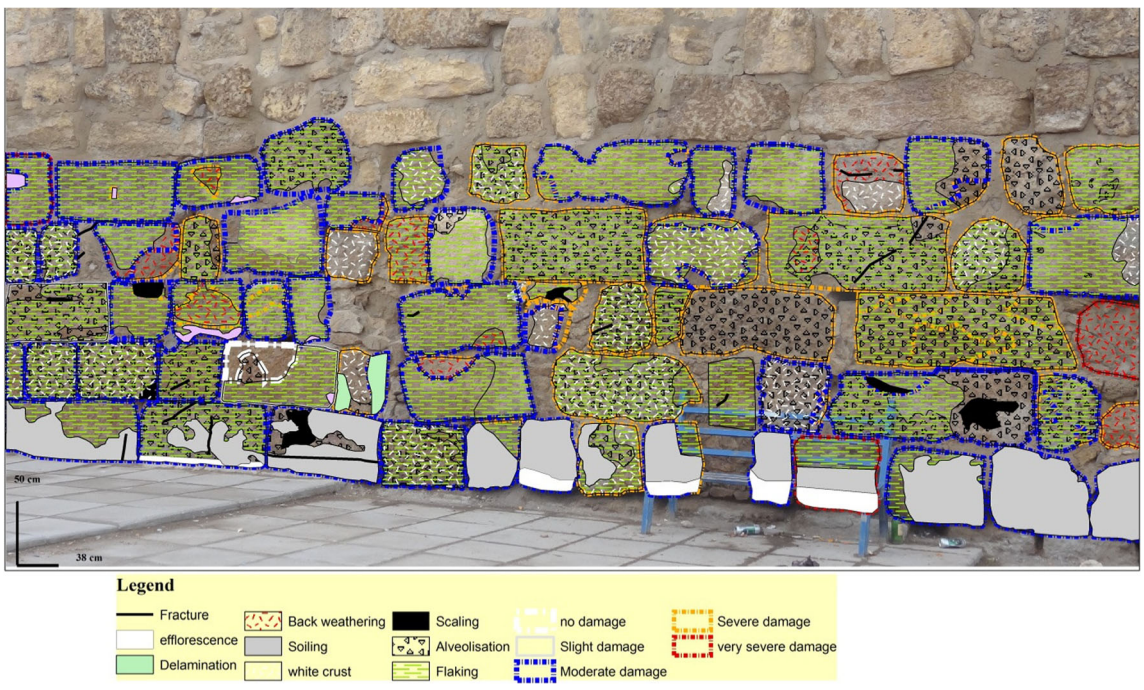

Fig. 6 Weathering forms obtained from the north side of the Byzantine Wall, which show only the limestones. The main weathering forms are flaking, alveolization, white crust, efflorescence, fracture, and discoloration. The damage categories of the Byzantine Wall are very severe, severe, moderate, slight and no damage

disaggregation, and the stones often present a great tendency to become discoloured.

X-ray diffraction and SEM analysis revealed that the efflorescence, white crusts and flaking are composed of gypsum and halite. The gypsum crystals are oriented at different angles to the surface of the pores (Fig. 7). The halite crystals present dissolution (corrosion) habits related to dissolution–precipitation cycles in the surface stone. The flakes, which are thin slivers of material that detach as salt crystallises behind them, are dominantly composed of gypsum. The detachment of the flakes suggests rhythmic fluctuations in the solution supply and salt crystallisation (Kramar et al. 2010). The fissures are 100–200 μm thick and oriented in different directions from the surface. The surface fissures present iron oxides and clay minerals and reduce the strength of the stone. The flow of water and salt solutions weakens the planes, and the cyclic swelling of clay contributes to the cracking and delamination of the stone (Rodriguez-Navarro et al. 1997; Sebastián et al. 2008).

Carbonate tufas represent approximately 50 stones in the entire Wall. This carbonate tufa generally presents two weathering forms, namely, loss of material (powdering and granular disaggregation) and fracturing when the stone is used in the lower part of the Wall close to the bottom. The investigation by the X-ray diffractometer for the weathering products shows salt absence. Meteoric waters may also have washed them out because they present high values of porosity and large pore sizes. Beyond a height of 5 m, no weathering forms appear in the stones, which tend to resist degradation at this height, whereas the weathering in the lower parts may be related to low mechanical resistance.

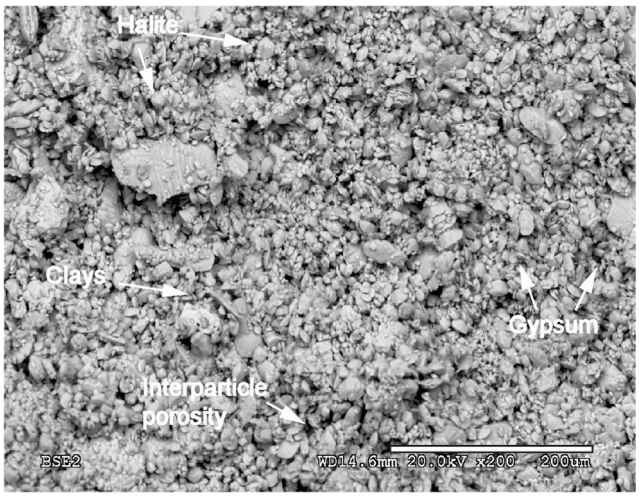

Fig. 7 Scanning electron microscopy (SEM) images for the weathered limestone surface. Gypsum crystals present a lenticular habit whereas halite crystals show dissolution forms. Interparticle porosity is partially closed by the clays and the salts

Damage categories are determined by comparing individual damage rates according to Fitzner and Heinrichs (2002) and Fitzner et al. (2002). The following five categories of damage were defined: very severe, severe, moderate, slight and no damage (Fig. 8). The Byzantine Wall revealed damage categories that range from moderate to severe. However, the most important weathering, including flaking, white crust, alveolisation, discolouration, granular disaggregation and back weathering, is found in the north and west facades. The weathering forms, which are recorded during the durability test, are showed in the Byzantine Wall for both stones, and mainly for flaking, alveolisation, efflorescence, fracture and loss of material.

Figure 8 shows the values of the Schmidt hammer rebound numbers obtained on weathered and unweathered surfaces. The differences between some of the Schmidt hammer rebound values can be explained by the differences in the values obtained from smooth surfaces, surfaces containing protruding grains and the fissured zone (Kolaitai and Papadopoulos 1993; Katz et al. 2000; Ericson 2004; Aydin 2009; Nazir et al. 2013; Sousa 2014). Furthermore, the values obtained from the Schmidt hammer test indicate changes in strength of the weathered and unweathered surfaces without any specific information about the weathering characteristics (Siedel et al. 2011).

Specifically, the surface strength decreases because of a loss of cohesion between grains. As a result, water can move easily within the pores and transport soluble salt, which is reflected by the flakes and surface deterioration (Mol 2014). The influences of water, porosity and mechanical strength changes result in the degradation of stones, which is reflected in the weathering forms. Finally, weathering generally affects limestone more than carbonate tufa because the weathering forms are controlled mainly by the lithology and the position of the stone within the Wall. These results were also reported

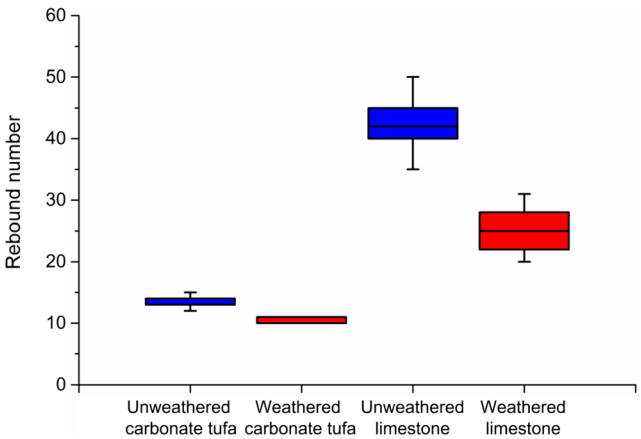

Fig. 8 Schmidt hammer rebound values of different conservation states, such as weathered and unweathered surfaces for limestone and carbonates tufa of the byzantine Wall

by Stück et al. (2011). Thus, the higher decay on the north face may be due to water, and that on the west face may be due to a higher thermal influence (Eppes et al. 2016) through salt action.

Conclusions

In this study, limestone and carbonate tufa showed several weathering forms, including flaking, alveolisation, efflorescence, discolouration, white crust, fracture, loss of materials and powdering. These weathering forms were mainly produced by salt action (gypsum and halite) as the result of interactions of multiple factors with a contribution of rising damp. Both stones were analysed and characterised via laboratory tests to understand stone durability. Limestone and tufa present different mineralogical, petrological and petrophysical properties that explain their behaviour in the constructions.

The porosity of limestone is lower than that of carbonate tufa, which is characterised by a specific macropore volume. This pore structure property is reflected in the capillary absorption coefficient. Because porosity strongly influences the mechanical properties, the P wave velocity and porosity display a negative linear relationship as pore space hinders the propagation of ultrasonic waves. Compressive strength and porosity exhibit a negative exponential trend. Limestones and tufas present a medium to very low resistance ranging from 56 to 70 MPa for limestones and from 1.5 to 3 MPa for carbonate tufas. The salt crystallisation test estimated the weathering processes as well as the petrophysical evolution of the stone response. Carbonate tufas show an excellent durability against salt crystallisation compared to the limestones.

Degradation and an increase in fissures were found on the surface of the stones. Bioturbation influences the porosity and iron oxide content of the stones, inducing granular disaggregation and brownish colours after contact with water. These weathering forms are accentuated by salt action and create fractures, flaking and more granular disaggregation. Mechanical strength is important in explaining the degradation in carbonate tufa, which has a very low resistance to loads, when used in the lower part of the Byzantine Wall. For carbonate tufas, there is a loss of salt constituents as the pore size is enormous and salt crystals are easily transported out of the stones. The failure of these stones in construction is due to their low resistance to compression. These stones failed easily and very quickly when used at the foot of the Byzantine Wall and remained intact when used in the upper rows.

In the Byzantine Wall, the damage ranges from medium to severe, demonstrating the inadequate conservation of the Byzantine Wall and the need for urgent preservation measures. The replacement of severely degraded stone is needed during the first steps of the conservation. This step will decrease the hazard of the structurural loss of stability of the Byzantine Wall. To limit the salt influence of the Wall, it is essential to prevent the water action and the rising damp. Finally, future deterioration of the built heritage of Tebessa is expected to be more substantial for limestone than carbonate tufa.

Acknowledgements The authors would like to thank all members of the Office for the Management and Exploitation of Protected Cultural Property, Algeria, for their permission for sampling in the Byzantine Wall. The authors would also like to acknowledge Martha Cary Eppes (University of North Carolina at Charlotte, USA), Andrea May (University of Muenster, Germany) and Djabri Rabah (University of Bejaia, Algeria) for their interesting suggestions and corrections of the manuscript.

References

Akin M, Özsan A (2011) Evaluation of the long-term durability of yellow travertine using accelerated weathering tests. Bull Eng Geol Environ 70:101–114https://doi.org/10.1007/s10064-010-0287-x

Allag L (2016) Analyse Petro-minéralogique et Sédimentaire du Turonien moyen- supérieur de Dj Essen (Région de Hammamet) en Atlas Saharien Oriental, Mémoire de Master, Université de Larbi Tbessi, Tebessa

Al Omari MMH, Rashid IS, Qinna NA, Jaber AM, Badwan AA (2016) Calcium Carbonate. In: Brittain HG (ed) Profiles of drug substances, excipients and related methodology, Vol. 41, Burlington: Academic, pp 31–132

ASTM (2001) Standard test method for determination of rock hardness by rebound hammer method. ASTM Stand. 04.09 (D 5873-00)

Aydin A (2009) ISRM suggested method for determination of the Schmidt hammer rebound hardness: revised version. Int J Rock Mech Min Sci 46:627–634

Beck K, Al-Mukhtar M (2010) Weathering effects in an urban environment: a case study of tuffeau, a French porous limestone. Geol Soc Lond Spec Pub 331:103–111. https://doi.org/10.1144/SP331.8

Benavente D (2011) Why pore size is important in the deterioration of porous stones used in the built heritage? Macla 15:41–42

Benavente D, García-del-Cura MA, Fort R, Ordóñez S (2004) Durability estimation of porous building stones from pore structure and strength. Eng Geol 74:113–127

Benavente D, Cueto N, Martínez-Martínez J, García Del Cura MA, Canãveras JC (2007a) The influence of petrophysical properties on the salt weathering of porous building rocks. Environ Geol 52:197–206. https://doi.org/10.1007/s00254-006-0475-y

Benavente D, Martínez-Martínez J, Cueto N, García-del-Cura MA (2007b) Salt weathering in dual-porosity building dolostones. Eng Geol 94:215–226

Benavente D, Sanchez-Moral S, Fernandez-Cortes A, JC C, Elez J, Saiz-Jimenez C (2011) Salt damage and microclimate in the Postumius tomb, Roman necropolis of Carmona, Spain. Environ Earth Sci 63: 1529–1543

Benavente D, Pla C, Cueto N, Galvañ S, Martínez-Martínez J, García-del-Cura MA, Ordóñez S (2015) Predicting water permeability in sedimentary rocks from capillary imbibition and pore structure. Eng Geol 195:301–311

Benavente D, Martínez-Martínez J, Cueto N, Ordóñez S, García Del Cura MA (2018) Impact of salt and frost weathering on the physical and durability properties of travertines and carbonate tufas used as building material. Environ Earth Sci 77:147. https://doi.org/10.1007/s12665-018-7339-0

Boumezbeur A, Hmaidia H, Belhocine B (2015) Limestone weathering and deterioration in the Tebessa Roman Wall NE Algeria. In:

Conference of Engineering Geology for Society and Territory 8: 169–174
Cassar J (2002) Deterioration of the Globigerina limestone of the Maltese islands. Geol Soc Lond Spec Pub 205:33–49. https://doi.org/10.1144/GSL.SP.2002.205.01.04
Cassar J, Galea M, Grima R, Stroud K, Torpiano A (2011) Shelters over the megalithic temples of Malta: debate, design and implementation. Environ Earth Sci 63:1849–1860. https://doi.org/10.1007/s12665-010-0735-8
Castel P (1912) Tébessa: Histoire et description d'un territoire algérien. Henri Paulin, Paris
Charola AE (2000) Salt in the deterioration of porous materials. J Am Inst Conserv 39:327–343. https://doi.org/10.2307/3179977
Coquand H (1862) Description géologique de la province de Constantine. Mémoires de la société géologique de France. Dagand, Bône
Deere DU, Miller RP (1966) Engineering classification and index properties for intact rock. Air Force Weapons Laboratory Technical, Report AFWL-TR-65-116
Doehne E (2002) Salt weathering: a selective review. Geol Soc Lond Spec Pub 205:51–64
Doehne E, Price CA (2010) The stone conservation: an overview of current research. Getty Conservation Institute, Los Angeles
Durozoy MG (1953) feuille n° 206, carte géologique et notice explicative, à 1/50000^{e}. Alger Serv Carte Géol, Algérie
Emmanuel S, Levenson Y (2014) Extreme limestone weathering rates due to micron-scale grain detachment. Geology. https://doi.org/10.1130/G35815.1
EN-12370 (1999) Natural stone test methods- Determination of resistance to salt crystallisation. 1999-03
EN-1926 (2007) UNE-EN 1926, 2007. Natural stone test methods. Determination of uniaxial compressive strength. AENOR, Madrid
Eppes MC, Griffing D (2010) Granular disintegration of marble in nature: a thermal-mechanical origin for a grus and corestone landscape. Geomorphology 117:170–180
Eppes MC, Keanini R (2017) Mechanical weathering and rock erosion by climate-dependent subcritical cracking. Rev Geophys. https://doi.org/10.1002/2017RG000557
Eppes MC, Magi B, Hallet E, Delmelle P, Mackenzie-Helnwein KW, Swami S (2016) Deciphering the role of solar-induced thermal stresses in rock weathering. Geol Soc Am Bull 128:1315–1338
Ericson K (2004) Geomorphological surfaces of different age and origin in granite landscapes: an evaluation of the Schmidt hammer test. Earth Surf Process Landf 29:495–509
Espinosa-Marzal RM, Scherer GW (2010) Mechanisms of damage by salt. Geol Soc Lond 33:61–77
Fitzner B, Heinrichs K (2002) Damage diagnosis on stone monuments—weathering forms, damage categories and damage indices. In: Přikryl R, Viles HA (eds) Understanding and managing stone decay. Karolinum, Prague, pp 11–56
Fitzner B, Heinrichs K, Kownatzki R (1995) Weathering forms— classification and mapping. In: Snethlage R (ed) Denkmalpflege und Naturwissenschaft, Natursteinkonservierung I. Ernst, Berlin, pp 41–88
Fitzner B, Heinrichs K, La Bouchardiere D (2002) Damage index for stone monuments. In: Galan E, Zezza F (ed) Protection and conservation of the cultural heritage of the mediterranean cities. Proceedings of the 5th international symposium on the conservation of monuments in the Mediterranean Basin, Sevilla, Spain, 5–8 April 2000. Swets and Zeitlinger, Lisse, pp 315–326
García-del-Cura MA, Benavente D, Martínez JM, Cueto N (2012) Sedimentary structures and physical properties of travertine and carbonate tufa building stone. Constr Build Mater 28:456–467
Garcia-Guinea J, Recio-Vazquez L, Almendros G, Benavente D, Correcher V, Perez-Garcia A, Sanchez-Moral S, Fernandez-Cortes A (2013) Petrophysical properties, composition and deterioration of the Calatorao biogenic stone: case of the sculptures masonry of the valley of the fallen (Madrid, Spain). Environ Earth Sci 69:1733–1750
Gomez-Heras M, McCabe S, Smith BJ, Fort R (2009) Impacts of fire on stone-built heritage an overview. J Architect Conserv 15:47–58
Gôtze J, Siedel H (2004) Microscopic scale characterization of ancient building sandstones from Saxony (Germany). Mater Charact 53: 209–222
Goudie AS, Viles HA (1997) Salt weathering hazards. Wiley, Chichester
Heinrichs, K (2008) Diagnosis of weathering damage on rock-cut monuments in Petra, Jordan. Environ Geol 56(3):643–675
ISRM (1978) Suggested methods for determining hardness and abrasiveness of rocks. Int J Rock Mech Min Sci Geomech Abstr 15:89–97
Jiménez González I, Scherer GW (2004) Effect of swelling inhibitors on the swelling and stress relaxation of clay bearing stones. Environ Geol 46:364–377
Katz O, Reches Z, Roegiers JC (2000) Evaluation of mechanical rock properties using a Schmidt hammer. Int J Rock Mech Min Sci 37: 723–728
Kolaitai E, Papadopoulos Z (1993) Evaluation of Schmidt rebound hammer testing: a critical approach. Bull IAEG 48:67–76
Koniorczyk M, Gawin D (2012) Modelling of salt crystallisation in building materials with microstructure-poromechanical approach. Constr Build Mater 36:860–873
Kramar S, Mladenović A, Urosevic M, Mauko A, Pristacz H, Mirtič B (2010) Deterioration of Lesno Brdo limestone on monuments (Ljubljana, Slovenia). RMZ-Mater Geoenviron:53–73
La Russa MF, Ruffolo SA, Belfiore CM, Aloise P, Randazzo L, Rovella N, Pezzino A, Montana G (2013) Study of the effects of salt crystallization on degradation of limestone rocks. Period Mineral 82: 113–127. https://doi.org/10.2451/2013PM007
López-Doncel R, Wedekind W, Leiser T, Molina-Maldonado S, Velasco-Sánchez A, Dohrmann R, Kral A, Wittenborn A, Aguillón-Robles A, Siegesmund S (2016) Salt bursting tests on volcanic tuff rocks from Mexico. Environ Earth Sci 75/212. https://doi.org/10.1007/s12665-015-4770-3
Malaga-Starzec K, Lindqvist JE, Schouenborg B (2002) Experimental study on the variation in porosity of marble as a function of temperature. Geol Soc Lond Spec Pub 205:81–88
Martínez-Martínez J (2008) Influencia de la alteración sobre las propiedades mecánicas de calizas, dolomías y mármoles. Evaluación mediante estimadores no destructivos (ultrasonidos). Dissertation, University of Alicante, Spain
Martínez-Martínez J, Benavente D, García-del-Cura MA (2011) Spatial attenuation: the most sensitive ultrasonic parameter for detecting petrographic features and decay processes in carbonate rocks. Eng Geol 119:84–95
May A (1994) Microfacies controls on weathering of carbonate building stones: Devonian (northern Sauerland, Germany). Facies 30:193–208
May A (1997) Verwitterungsbeständigkeit und Verwitterung von Naturbausteinen aus Kalkstein. Geologie und Paläontologie in Westfalen, Münster
May A (1998a) Die Verwitterung von karbonatischen Naturbausteinen in Mitteleuropa. Geookodynamik 19:71–88
May A (1998b) Verwitterung und Verwitterungsbeständigkeit von Naturbausteinen aus Kalkstein am Beispiel des Osnabrücker Wellenkalks (Trias). Jb Geol Paläont 208:637–651
McCabe S, Smith BJ, Warke PA (2007) Preliminary observations on the impact of complex stress histories on sandstone response to salt weathering: laboratory simulations of process combinations. Environ Geol 52:251–258
Mol L (2014) Measuring rock hardness in the field. In: Clarke LE, Nield JM (eds) . Geomorphological Techniques (Online Edition). British Society for Geomorphology, London, pp 1–8
Nazir R, Momeni E, Jahed Armaghani D, Mohd Amin MF (2013) Prediction of unconfined compressive strength of limestone rock

samples using Ltype Schmidt hammer. Electr J Geotech Eng 18: 1767–1775
Nicholson DT (2001) Pore properties as indicators of breakdown mechanisms in experimentally weathered limestones. Earth Surf Proc Land 26:819–838. https://doi.org/10.1002/esp.228
Price CA (1975) Stone decay and preservation. Chem Br 11:350–353
Price C (2006) Consolidation. In: Henry A (ed) Stone conservation: principles and practice. Donhead, Shaftesbury, 101–126
Price C (2007) Predicting environmental conditions to minimise salt damage at the tower of London: a comparison of two approaches. Environ Geol 52:369–374
Přikryl R, Weishauptová Z, Novotná M, Přikrylová J, Št'astná A (2010) Physical and mechanical properties of the repaired sandstone ashlars in the facing masonry of the Charles bridge in Prague (Czech Republic) and an analytical study for the causes of its rapid decay. Environ Earth Sci. https://doi.org/10.1007/s12665-010-0819-5
Queisser A (1986) Geotechnische und mineralogische Bewertung von Natursandsteinen aus dem Raum Bamberg. Dissertation, Johannes Gutenberg-Universität
Rodriguez-Navarro C, Hansen E, Sebastián E, Ginell W (1997) The role of clays in the decay of ancient Egyptian limestone sculptures. J Am Inst Cons 36:151–163. https://doi.org/10.2307/3179829
Ruedrich J, Kirchner D, Siegesmund S (2011) Physical weathering of building stones induced by freeze–thaw action: a laboratory long-term study. Environ Earth Sci 63:1573–1586. https://doi.org/10.1007/s12665-010-0826-6
Ruffolo SA, La Russa MF, Aloise P, Belfiore CM, Macchia A, Pezzino A, Crisci GM (2013) Efficacy of nanolime in restoration procedures of salt weathered limestone rock. Appl Phys A 114:753–758
Ruffolo SA, Comite V, La Russa MF, Belfiore CM, Barca D, Bonazza A, Crisci GM, Pezzino A, Sabbioni C (2015a) Analysis of black crusts from the Seville cathedral: a challenge to deepen understanding the relationship among microstructure, microchemical features and pollution sources. Sci Total Environ 502:157–166
Ruffolo SA, La Russa MF, Ricca M, Belfiore CM, Macchia A, Comite V, Pezzino A, Crisci GM (2015b) New insights on the consolidation of salt weathered limestone: the case study of Modica stone. Bull Eng Geol Environ. https://doi.org/10.1007/s10064-015-0782-1
Schaffer RJ (1932) The natural weathering of building stones. HMSO, London
Schneider C, Ziesch J, Bauer A, TÖRÖT A, Siegesmund S (2008) Bauwerkskartierung zur Analyse des Verwitterungsstatus an den Außenmauern des Schlosses von Buda (Budapest, Ungarn). Schriftenr Deutsch Ges Geowissensch 59:209–225
Sebastián E, Cultrone G, Benavente D, Linares Fernandez L, Elert K, Rodriguez-Navarro C (2008) Swelling damage in clay-rich sandstones used in the church of San Mateo in Tarifa (Spain). J Cult Herit 9:66–76
Siedel H, Siegfried S, Sterflinger K (2011) Characterization of stone deterioration on buildings. In: Siegesmund and Snethlage (ed) stone in architecture, 4th edn. Springer, Berlin, pp 347–410. https://doi.org/10.1007/978-3-642-14475-2_6
Siegesmund S, Dürrast H (2011) Physical and Mechanical Properties of Rocks. In: S. Siegesmund, R. Snethlage (eds.), Stone in Architecture, 4th ed., 97-226. https://doi.org/10.1007/978-3-642-14475-2_3
Siegesmund S, Török A (2011) Building stones. In: Siegesmund S, Snethlage R (eds) Stone in architecture—properties, durability, 4th edn. Springer, Berlin, pp 11–96. https://doi.org/10.1007/978-3-642-14475-2_2
Smith BJ, Gomez-Heras M, Viles AH, Cassar J (2010) Limestone in the built environment: present-day challenges for the preservation of the past. Geol Soc Lond Spec Publ 331
Sousa LMO (2014) Petrophysical properties and durability of granites employed as building stone: a comprehensive evaluation. Bull Eng Geol Environ 73:569–588. https://doi.org/10.1007/s10064-013-0553-9
Stück H, Siegesmund S, Ruedrich J (2011) Weathering behaviour and construction suitability of dimension stones from the Drei Gleichen area (Thuringia, Germany). Environ Earth Sci 63:1763–1786. https://doi.org/10.1007/s12665-011-1043-7
Thomachot C, Jeannette D (2002) Evolution of the petrophysical properties of two types of Alsatian sandstone subjected to simulated freeze-thaw conditions. Geol Soc Lond, Spec Publ 205:19–32
Török A (2006) Influence of fabric on the physical properties of limestones. In: Kourkoulis SK (ed) Fracture and failure of natural building stones. Springer, Dordrecht, pp 487–495
UNE EN-1925 (1999) UNE-EN 1925 (1999) Natural stone test methods. Determination of water absorption coefficient by capillarity
UNE-EN 1936 (2007) Natural stone test methods. Determination of real density and apparent density, and of total and open porosity. AENOR, Madrid
Winkler EM (1997) Stone in architecture. Properties, durability, 3rd edn. Springer, Berlin
Yu S, Oguchi CT (2010) Role of pore size distribution in salt uptake, damage, and predicting salt susceptibility of eight types of Japanese building stones. Eng Geol 115:226–236